Title
THE CO-PRECIPITATION OF VACANCIES AND CARBON ATOMS IN QUENCHED PLATINUM

Author
Westmacott, K.H.

Publication Date
1979

Submitted to Journal of Nuclear Material

THE CO-PRECIPITATION OF VACANCIES AND CARBON ATOMS IN QUENCHED PLATINUM

K. H. Westmacott and M. I. Perez

January 1979

Prepared for the U. S. Department of Energy
under Contract W-7405-ENG-48

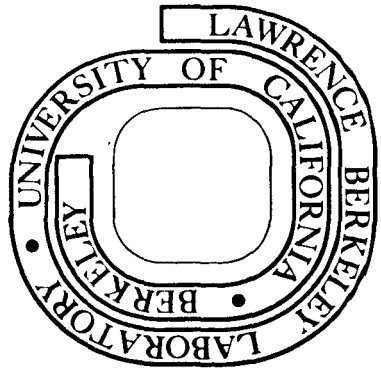

DISCLAIMER

THE CO-PRECIPITATION OF VACANCIES AND CARBON ATOMS IN QUENCHED PLATINUM*

K. H. Westmacott and M. I. Perez

Materials and Molecular Research Division
Lawrence Berkeley Laboratory
Berkeley, California 94720

ABSTRACT

The geometry of secondary defect structures observed in quenched platinum containing various amounts of carbon is shown to be consistent with a simple model based on the premise of a strong impurity (carbon) atom/vacancy binding energy. When the ratio of carbon atoms to vacancies (C_c/C_v) is large, co-precipitation as platelets on {100} planes occurs; whereas when C_c/C_v is small the effects of carbon are still manifest but the defect geometry is dominated by the vacancy behavior, and loops on {111} planes form. Consideration of the mechanism of defect formation on {100} planes leads to conclusions about the structure of the carbon atom/vacancy complex, its migration and stability. An electron microscopy analysis of the {100} defects is in excellent accord with the proposed model. Implications concerning the likely behavior of carbon atoms in a radiation environment are considered, and an interstitial impurity solute segregation effect to vacancy sinks is predicted.

*This work was supported by the Division of Materials Sciences, Office of Basic Energy Sciences, U.S. Department of Energy.

1. Introduction

Quenching experiments performed under well-controlled conditions can provide direct information on vacancy clustering and vacancy/impurity interactions. For example, recent transmission electron microscopy studies [1] using an ultrahigh vacuum quenching apparatus [2] which allowed quenching from pressures < 1μPa have shown that vacancy clustering in FCC metals is strongly influenced by the presence of interstitial impurities, especially carbon and oxygen. Striking variations in the defect structure were observed in a series of platinum specimens of various purity quenched from different temperatures and explained in terms of strong carbon atom/vacancy interaction and changes in the ratio of the number of carbon atoms to vacancies.

In the least pure platinum studied, co-precipitation of the carbon and vacancies occurred as platelets of {100} planes, whereas in the purest platinum vacancy loops formed on the usual {111} planes. In the present paper a simple hard-sphere model is developed that accounts for {100} loop formation, and a detailed TEM contrast analysis of the defects is in excellent accord with the proposed model.

Implications regarding the nature of the diffusing complex follow that have a bearing on the question of solute segregation in alloys irradiated in a reactor, and provide further evidence that interstitial as well as substitutional impurity atoms can be redistributed under appropriate conditions.

2. A Model for the Formation of {100} Loops

In FCC metals interstitial impurity atoms normally occupy $0,0,\frac{1}{2}$, type octahedral interstitial sites and have 6 metal atom nearest neighbors. On the basis of a simple hard-sphere model, these positions can be occupied

without lattice strain only if the impurity/metal atom size ratio, $R_s/R_m \leq 0.41$. For the case of carbon in platinum $R_s/R_m = 0.56$, thus it is $\sim$ 37% oversize. In Table 1 atomic misfits for carbon and other interstitial impurities in the FCC metals are given, and it is seen that, with the exception of Th, the strain associated with C is large in all the metals listed. In simple terms, this elastic strain energy forms the basis for understanding the experimental observations that carbon atoms nucleate vacancy clusters in FCC metals [1].

Let us now consider the situation following a rapid quench from a high temperature to near ambient temperatures in which both vacancies and carbon atoms are highly supersaturated. These conditions are satisified for Pt containing relatively small amounts of C, as may be seen from the solubility and vacancy concentration data presented in Fig. 1. In the present work platinum containing 800 appm was quenched from 1250°C to 400°C. Under these conditions the equilibrium vacancy concentration at 1250°C is 4×10^{-5}, $C_c = 8 \times 10^{-4}$, and $C_c/C_v \simeq 20$, whereas the vacancy and carbon equilibrium concentrations at 400°C are 2.5×10^{-11} and 1.6×10^{-5} giving rise to supersaturations of 2×10^6 and 50 respectively. Thus, precipitation of both vacancies and carbon should occur. Consideration of the geometric possibilities for carbon/vacancy co-precipitation in the FCC lattice leads to a probable mechanism for dislocation loop/carbon platelet formation on {100} planes. If a quenched-in vacancy arrives as a nearest neighbor to an interstitial carbon atom, the carbon can eliminate its lattice strain energy simply by jumping into the vacant lattice site*, i.e., by jumping from an interstitial to a substitutional site. Since this is an energetically favorable process,

*The relaxation volume of a vacancy in Pt has been determined experimentally to be 0.33Ω[6]; nevertheless, the residual hole is still much larger than the carbon atom.

in the case under consideration where $C_c/C_v = 20$, all the vacancies will acquire a carbon atom. If we now compare the precipitation of these vacancy/carbon complexes with normal vacancy precipitation it is clear that because the formation of a Frank dislocation loop on a {111} plane maintains close packing of the atoms, complete collapse to form a stable defect with b = a/3 <111> can occur only by forcing the associated carbon atoms back onto interstitial sites with a consequent increase in the total energy of the configuration. The same considerations apply to the precipitation of perfect loops with b=a/2<110> on {111} or {110} planes. On the other hand, if precipitation occurs on {100} planes the limited relaxation of atoms in the <100> directions due to contact between adjacent atoms (see Fig. 2) still leaves holes in the lattice sufficiently large to accommodate the carbon atoms without introducing lattice strain. The sequence of atomic configurations before and after collapse of a vacancy/carbon disc on (100) is shown schematically in Figure 2. The minimum diameter of the residual hole in a {100} loop is given by $d=(a^2 + b^2)^{\frac{1}{2}} - b = 0.52a$, where a is the lattice constant, and b the Burgers vector. The value of d for platinum is 2.04Å, which may be compared with the carbon atom diameter of 1.54Å.

The (100) configuration shown in Fig. 2(d) consists of an imperfect dislocation loop with Burgers vector of magnitude $|b| = (a-b) \simeq 0.3a$, therefore $\underline{b} \simeq a/3$ [100]. The resulting stacking fault is a high energy configuration analogous to A-A stacking in the normal {111} plane stacking sequence, but because of the ready accommodation of the carbon atoms in the structure it is apparently the most favorable arrangement. Its displacement vector, R, is also 0.3a [100] and like $\underline{b}$ is unusual since it is a non-rational fraction of a lattice vector. However, it is close enough to a/3 [100] for the fault and loop to exhibit near invisibility under the appropriate

diffraction conditions. In the following section this model is compared with the experimentally determined contrast behavior.

3. Results

The quenching and thin-foil preparation techniques used in the experiments together with some of the experimental results have been described in detail previously [1].

Several grades of Pt were studied, but the results from only two are reported here; an impure grade containing (in appm) 3000 Rh, 950 Pd, 300 Ir, 140 Si, 70 Fe, and 800 C, and Pt supplied by Materials Research Corporation containing 40 Rh, 52 Fe, 70 Si, 5 Ag, 20 Ti, and 80 C. Disregarding the soluble substitutional impurities, all of which are well within the solubility limits at all temperatures, the principal difference between the two materials is the order of magnitude change in the carbon content. Since many quenching studies have shown that the presence of small concentrations of substitutional impurities does not affect the type of secondary defect formed, the results below are attributed to these differences in carbon content.

In summary the observations have shown that:

(i) Planar defects which show fringe contrast and lie on {100} planes are formed after quenching Pt containing 800 appm carbon from the temperature range 1000-1760°C. These platelet defects which are believed to be associated with the carbon impurities, are best observed in foils quenched from 1250°C into a salt bath at 400°C, and in specimens quenched from 1760°C at a slower rate in the UHV quenching apparatus. Dislocation decoration, platelet formation on dislocations and associated denuded zones are also observed.

(ii) In purer Pt containing ~80 appm C, "normal" dislocation loops lying on {111} planes with $\underline{b}$ = a/3 <111> or a/2 <110> are observed in specimens quenched from 1760°C.

3.1 Contrast Analysis

A detailed contrast analysis has been made on the {100} defects and the series of micrographs given in Fig. 3 typify the results. Assuming that the simple results of contrast theory [7] are valid for {100} loops with b = R $\simeq$ a/3 <100> the predicted behavior under various diffraction conditions is given in Table 2. A consistent agreement is found between the predictions of the model and the experimental data indicating that the breakdown in the invisibility criterion and other complexities that can arise in the contrast analysis of partial dislocations [8] do not occur.* For example, Fig. 3 (a) taken with a beam direction, $\underline{B}$ = [121] and diffraction vector, $\underline{g}$, = $[1\bar{1}1]$ shows all three sets of loops on the {100} planes. The faults in each case are visible since $\alpha = 2\pi/3$, but the dislocations are not, since $\underline{g} \cdot \underline{b} = 1/3$. On the otherhand, when $\underline{B}$ = [011] and $\underline{g}$ = 200 (see Fig. 3(b)) only the set of loops edge on with R = a/3 [100] is seen; the other two sets are invisible since both $\underline{g} \cdot \underline{b}$ and α are zero. With $\underline{B}$ = [011] and $\underline{g} = \bar{1}\bar{3}\bar{3}$, (Fig. 3(c)) one set of loops is again edge on, while the other two sets make equal inclination to the beam; for these sets $\alpha = 2\pi$ and no fault contrast is observed whereas $\underline{g} \cdot \underline{b} = \pm 1$ and the dislocations are in strong contrast. Finally, with $\underline{B}$ = [111] and $\underline{g} = [\bar{2}02]$ (see Fig. 3(d)) the observed contrast behavior is again in accordance with the predictions of Table 2.

4. Discussion

Detailed contrast experiments presented here suggest that {100} loops in Pt have a Burgers vector, $\underline{b}$, and fault displacement vector, $\underline{R}$, $\simeq$ a/3 <100>, while previous work [1] has shown they are intrinsic in nature, which

---

*This may be because the line segments comprising {100} loops are pure edge and lie along <100> which are normal to the elastic symmetry plane. Thus, pseudo-isotropic behavior is expected.

indicates that they form by a vacancy mechanism. This is in complete agreement with the model presented in section 2.

Several aspects of these {100} defects warrant discussion. They are particularly stable defects as evidenced by the observation that they are unaffected by intersection with the foil surfaces, a process which normally results in unfaulting. Unfaulting by shear to form a perfect loop with b = a/2 [110] cannot occur, however, for the same reason that {110} loops cannot form in the first place, namely, the shear process would have to be accompanied by a return of carbon atoms to interstitial sites. This accounts for the unusally high stability of the {100} loops in contrast to the {111} loops found in other FCC metals.

The observation that {100} loops are still formed in the impure Pt quenched from close to the melting point is consistent with the model since $C_v(1760) \simeq 8 \times 10^{-4}$, giving $C_c/C_v \sim 1$, i.e., there is still approximately one carbon atom per vacancy. On the otherhand, in the purer platinum containing 80 appm C, $C_c/C_v \sim 1/10$ and loops are now observed to be on the usual {111} planes.

Since previous work [1] has shown that there is a gradual transition in the observed defect structure from vacancy/carbon co-precipitation to pure vacancy precipitation as the ratio of carbon to vacancies is decreased, it is reasonable to assume that every vacancy precipitated in a {100} loop has an associated carbon atom. It then follows that the complex must have migrated as an entity by a process where dissociative jumps are improbable or transitory. It is interesting to compare these deductions with theoretical predictions. Beeler [9] has performed computer simulation studies of various point defect-carbon atom configurations in the nickel lattice and found quite large positive binding energies for several complexes. Values of 0.30 and 0.86 ev were estimated for a monovacancy-carbon and divacancy-carbon complex

respectively, and the most stable monovacancy complex is one in which the carbon atom and vacancy lie at a distance of 0.2a from each other in a {100} plane. In more recent work [10] he has also discussed the probable paths the complex takes during migration. The mechanism of {100} loop formation which follows from both theory and experiment is therefore one in which isolated carbon atoms strongly interact with vacancies to form a complex with the carbon effectively in a substitutional site. This complex can migrate readily and precipitate at normal vacancy sinks such as free surfaces, grain boundaries, dislocations or other vacancy clusters. Consequently, carbon present in supersaturated solution in a metal containing a high mobile vacancy flux as a result of, for example, quenching, or exposure in a nuclear reactor, would be expected to undergo extensive redistribution, i.e., interstitial impurity solute segregation will occur. As shown in Table I, of the other common interstitial impurities, only oxygen would be expected to behave similarly in appropriate metals. Recent experimental evidence from both quenching and irradiation experiments suggest that the present conclusions may also be valid for BCC metals. For example, Dahmen and Thomas [11] in a study of quenched Ta containing C have observed {310} loops resulting apparently from carbon/vacancy co-precipitation. Weber et al., [12] reported that in ion-irradiation vanadium, interstitial carbon precipitated as VC by a mechanism assumed to be associated with solute segregation. Agarwal and Taylor [13] reported similar effects and suggested that the precipitation of VC consumes vacancies that would otherwise increase the swelling. Loomis et al., [14] have shown that the presence of 500 appm O in Nb reduces swelling and promotes void ordering. There is therefore a growing body of evidence that interstitial impurity/point defect interactions may strongly influence radiation behavior in both FCC and BCC materials. Finally, if vacancies and carbon atoms co-precipitate under irradiation conditions such a "carbon

saturated" loop will have a greater stability than a pure vacancy loop because, (1) additional energy is required to return a carbon atom to solution when an interstitial atom annihilates at the loop and (2) the loop remains sessile. This implies that the dislocation loop bias factor will be reduced and the loop lifetime will be increased, both of which should lead to reduced swelling. Recent work by Sorenson and Chen [15] has in fact shown that void swelling in Ni is progressively reduced as the carbon content is increased. These authors attributed the decrease in swelling to a dynamic trapping mechanism involving carbon atoms and vacancies. However, the present work suggests static trapping at carbon/vacancy clusters may be occurring.

Acknowledgements

This work was supported by the Division of Materials Sciences, Office of Basic Energy Sciences, U.S. Department of Energy. The authors thank Prof. J. R. Beeler, Jr., for supplying pre-publication results.

FIGURE CAPTIONS

Fig. 1. Graph of carbon and vacancy concentration as a function of temperature. Two alternative curves for the carbon solubility [3,4] are plotted but the present work is based on, and in accord with, the data of Selman et al., [3] as reported in [5].

Fig. 2. Schematic representation of the sequence of events leading to the formation of {100} defects: (a) isolated vacancies and interstitial carbon, (b) vacancy/carbon complex formation, (c) co-precipitation as platelet on {100} planes, (d) final configuration after lattice relaxation to form an a/3 [100] loop.

Fig. 3. Series of micrographs illustrating diffraction contrast behavior of {100} defects. See text for detailed interpretation. The diffraction conditions are (a) $\underline{B}$ = [121], $\underline{g}$ = $[1\bar{1}1]$, $\underline{w}$ = 0.2; (b) $\underline{B}$ = [011] , $\underline{g}$ = 200, $\underline{w}$ = 0.2; (c) $\underline{B}$ = [011], $\underline{g}$ = $[\bar{1}33]$, $\underline{w}$ = 1.0; (d) $\underline{B}$ = [111], $\underline{g}$ = $[\bar{2}02]$, $\underline{w}$ = 0.6.

REFERENCES

[1]. K. H. Westmacott, Cryst. Lattice Defects, 6 (1976) 203.

[2]. K. H. Westmacott and R. L. Peck, J. Phys. E. Scient. Instr., 9 (1976) 21.

[3]. G. L. Selman, P. J. Ellison and A. S. Darling, Platinum Met. Rev. 14 (1970) 14.

[4]. R. H. Siller, W. A. Oates and R. B. McLellan, J. Less-Comm. Met. 16 (1968) 71.

[5]. Gase Und Kohlenstoff in Metallen (Springer, Berlin 1976) p. 650.

[6]. M. Charles, J. Hillairet, M. Beyeler and J. Delaplace, Phys. Rev. B11 (1975) 71.

[7]. P. B. Hirsch, A. Howie, R. B. Nicholson, D. W. Pashley and M. J. Whelan, Electron Microscopy of Thin Crystals (Butterworth, London (1967) p. 165-172.

[8]. J. W. Edington, Practical Electron Microscopy in Materials Science, Philips Tech. Lib. 3 (1975) p. 19.

[9]. J. R. Beeler, Jr. Interatomic Potentials and Simulation of Lattice Defects (Plenum Press, New York 1972) p. 339.

[10]. J. R. Beeler, Jr., private communication.

[11]. U. Dahmen and G. Thomas, private communication.

[12]. W. J. Weber, G. L. Kulcinski, R. G. Lott, P. Wilkes and H. V. Smith, Radiation Effects and Tritium Technology for Fusion Reactor, Gatlinburg Conference-750989 I (1975) p. 130.

[13]. S. C. Agarwal and A. Taylor, Radiation Effects and Tritium Technology for Fusion Reactor, Gatlinburg Conference-750989 I (1975) p. 150.

[14]. B. A. Loomis, A. Taylor and S. B. Gerber, Radiation Effects and Tritium Technology for Fusion Reactor, Gatlinburg Conference-750989 I (1975) p. 93.

[15]. S. M. Sorenson and C. W. Chen, Radiation Effects 33 (1977) 109.

TABLE I

ATOMIC MISFIT VALUES FOR INTERSTITIAL ATOMS IN FCC METALS

SOLVENT METAL	Rs (Å) / Rm (Å)	CARBON=0.77		OXYGEN=0.65		NITROGEN=0.53		HYDROGEN=0.37	
		Rs/Rm	%O-SIZE	Rs/Rm	%O-SIZE	Rs/Rm	%O-Size	Rm/Rs	%O-SIZE
NICKEL	1.24	0.62	51	0.52	27	0.43	5	0.30	-27
COPPER	1.27	0.61	49	0.51	24	0.42	2	0.29	-29
γ-IRON	1.29	0.60	46	0.50	22	0.41	0	0.29	-29
PLATINUM	1.38	0.56	37	0.47	15	0.38	-7	0.27	-34
ALUMINUM	1.43	0.54	32	0.45	10	0.37	-10	0.26	-32
SILVER	1.44	0.53	29	0.45	10	0.37	-10	0.26	-37
GOLD	1.44	0.53	29	0.45	10	0.37	-10	0.26	-37
THORIUM	1.80	0.43	5	0.36	-12	0.29	-29	0.21	-49

TABLE II

VALUES OF $\underline{g} \cdot b$ AND α ($= 2\pi \underline{g} \cdot \underline{R}$) FOR a/3 <100> LOOPS

$\underline{g}$	$\underline{b} = \pm 1/3$ [100]	$\underline{b} = \pm 1/3$ [010]	$\underline{b} = \pm 1/3$ [001]	$\underline{R} = 1/3$ [100]	$\underline{R} = 1/3$ [010]	$\underline{R} = 1/3$ [001]
$1\bar{1}1$	$\pm$ 1/3 (I)	$\pm$ 1/3 (I)	$\pm$ 1/3 (I)	$2\pi/3$ (V)	$2\pi/3$ (V)	$2\pi/3$ (V)
200	$\pm$ 2/3 (V/I)	0 (I)	0 (I)	$4\pi/3$ (V)	0 (I)	0 (I)
$\bar{2}02$	$\pm$ 2/3 (V/I)	0 (I)	$\pm$ 2/3 (V/I)	$-4\pi/3$ (V)	0 (I)	$4\pi/3$ (V)
$\bar{1}\bar{3}3$	$\pm$ 1/3 (I)	$\pm$ 1 (V)	$\pm$ 1 (V)	$-2\pi/3$ (V)	2π (I)	2π (I)

(V): DISLOCATION LOOP OR STACKING FAULT IN STRONG CONTRAST

(I): DISLOCATION LOOP OR STACKING FAULT IN WEAK CONTRAST

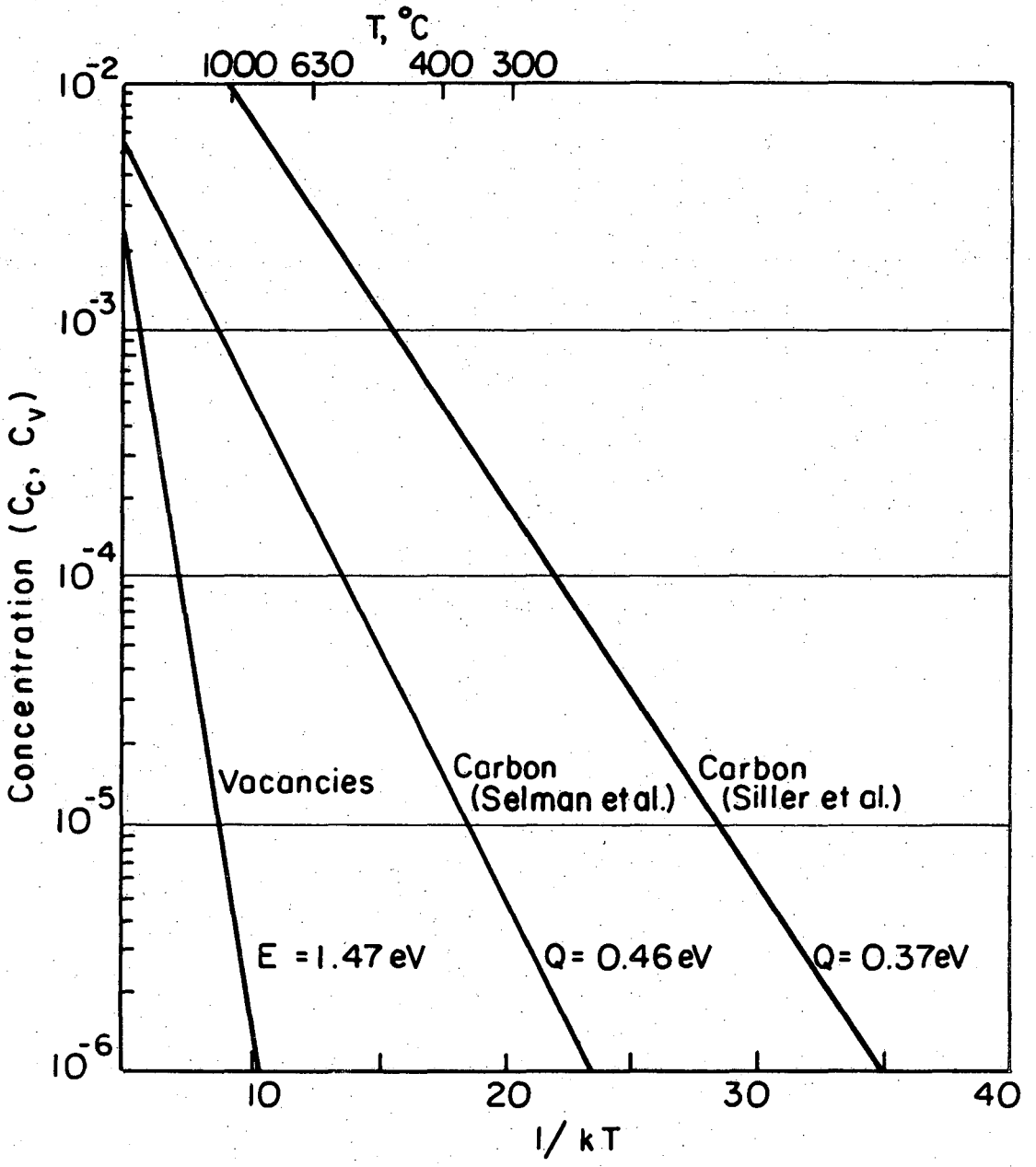
T, °C
1000 630 400 300
10^{-2}
10^{-3}
10^{-4}
10^{-5}
10^{-6}
Concentration (C_c, C_v)
Vacancies
Carbon (Selman et al.)
Carbon (Siller et al.)
E = 1.47 eV
Q = 0.46 eV
Q = 0.37 eV
10
20
30
40
1/ kT
XBL789-5815

Fig. 1

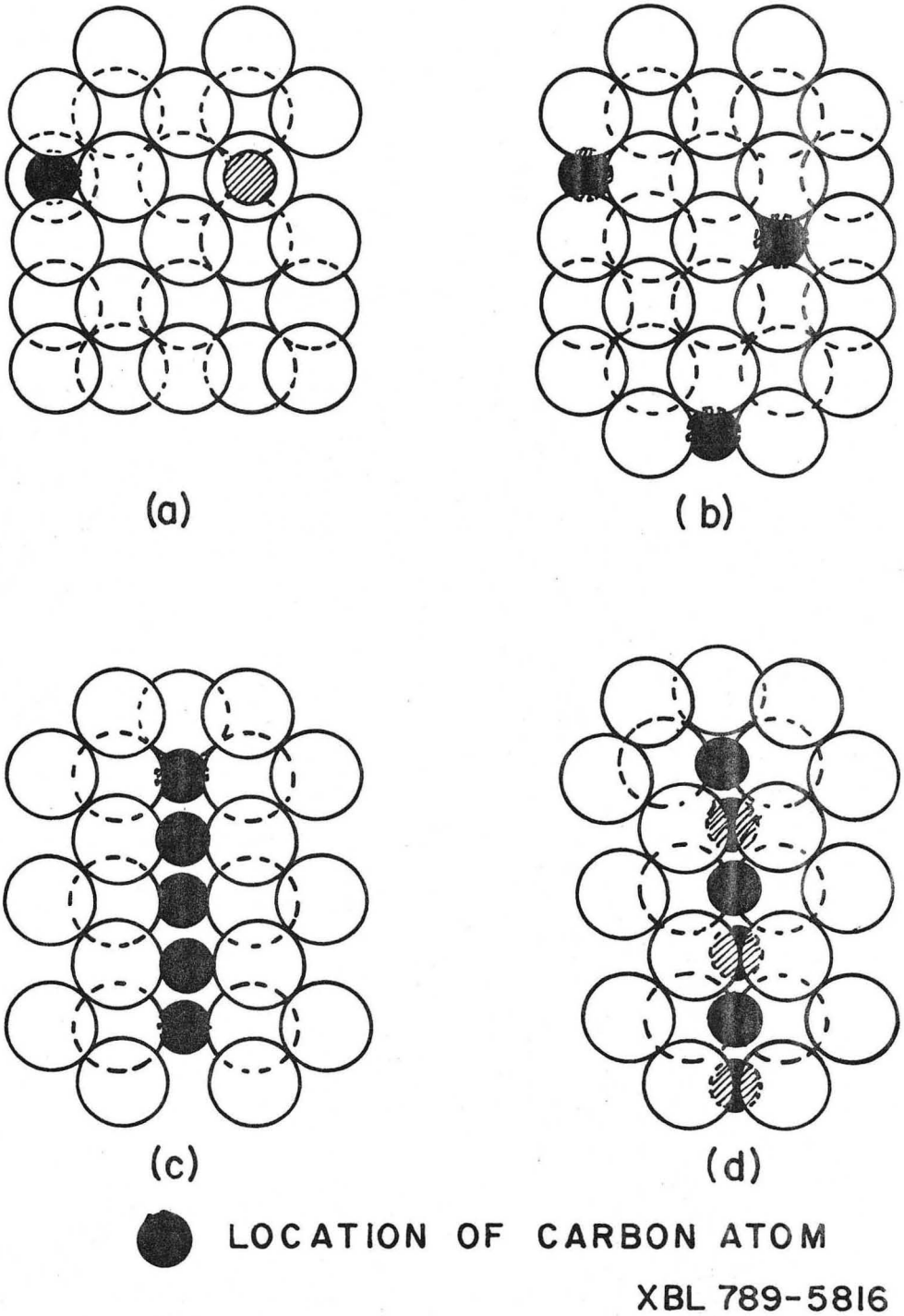

Fig. 2

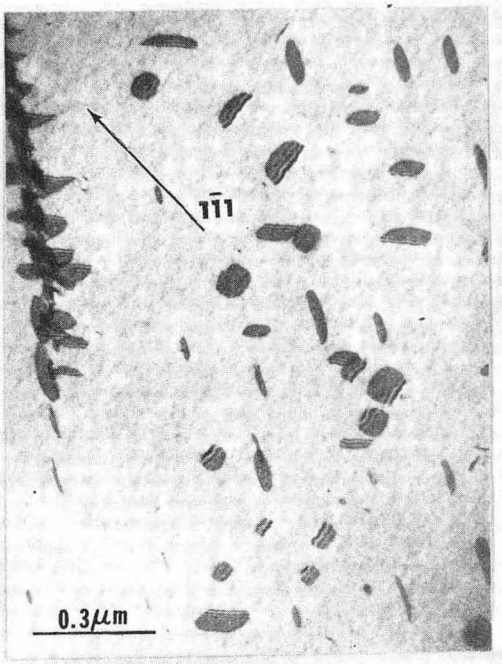

Fig. 3(a)

Fig. 3(b)

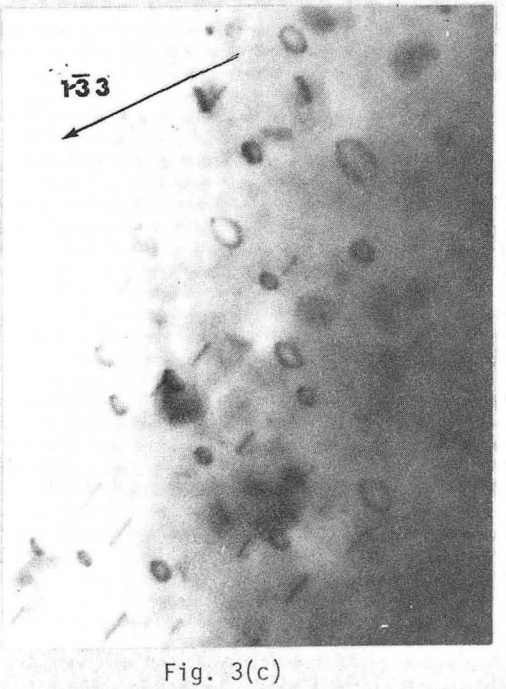

Fig. 3(c)

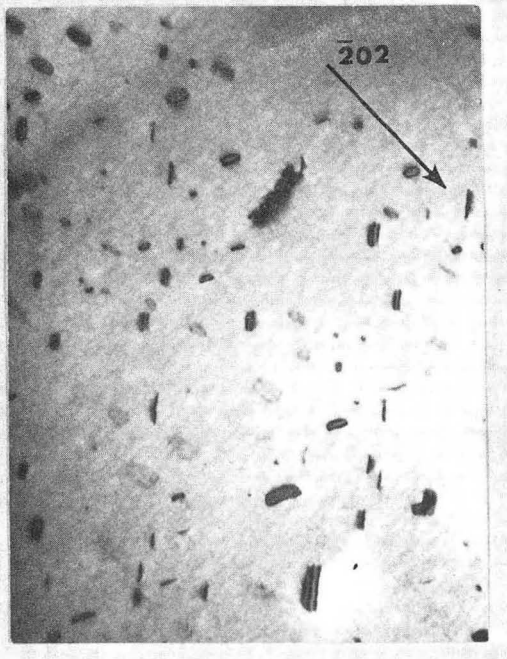

Fig. 3(d)

FIGURE 3

This report was done with support from the Department of Energy. Any conclusions or opinions expressed in this report represent solely those of the author(s) and not necessarily those of The Regents of the University of California, the Lawrence Berkeley Laboratory or the Department of Energy.

TECHNICAL INFORMATION DEPARTMENT
LAWRENCE BERKELEY LABORATORY
UNIVERSITY OF CALIFORNIA
BERKELEY, CALIFORNIA 94720